Bromodomain and Extraterminal Domain Inhibition Synergizes with WEE1-Inhibitor AZD1775 Effect by Impairing Non-Homologous End Joining and Enhancing DNA Damage in Non-Small Cell Lung Cancer

Yuta Takashima[1], Eiki Kikuchi[1*], Junko Kikuchi[1], Motofumi Suzuki[2], Hajime Kikuchi[1,3], Makie Maeda[1], Tetsuaki Shoji[1], Megumi Furuta[1], Ichiro Kinoshita[4], Hirotoshi Dosaka-Akita[4], Jun Sakakibara-Konishi[1], Satoshi Konno[1]

[1] Department of Respiratory Medicine, Faculty of Medicine and Graduate School of Medicine, Hokkaido University, Sapporo, Japan
[2] Laboratory for Bioanalysis and Molecular Imaging, Graduate School of Pharmaceutical Sciences, Hokkaido University, Sapporo, Japan
[3] First Department of Medicine, JA Obihiro Kosei Hospital, Obihiro, Japan
[4] Department of Medical Oncology, Faculty of Medicine and Graduate School of Medicine, Hokkaido University, Sapporo, Japan

Running title: BET and WEE1 inhibition in non-small cell lung cancer
Keywords: BET bromodomain inhibitor, WEE1 inhibitor, DNA damage repair, non-homologous end joining, non-small cell lung cancer
Article category: Molecular Cancer Biology

Abbreviations: BET: Bromodomain and extraterminal domain; CI: Combination index; CtIP: C-terminal binding protein interacting protein; DNA-PKcs: DNA-dependent protein kinase catalytic subunit; DSB: Double-strand break; HR: Homologous recombination; MYT1: Myelin transcription factor 1; NHEJ: Non-homologous end joining; NSCLC: Non-small cell lung cancer; pHH3: Phospho histone H3; PI: Propidium Iodide; P-TEFb: Positive transcription elongation factor b; qRT-PCR: Quantitative reverse transcription PCR

Novelty and impact: We show that combined inhibition of BET and WEE1 synergistically suppresses NSCLC growth. BET inhibition considerably repressed NHEJ pathway-related genes and diminished NHEJ pathway-mediated DNA double-strand break repair. Furthermore, BET inhibition repressed MYT1 expression and promoted mitotic entry when combined with WEE1 inhibition. This is the first report to show that BET inhibition synergizes with WEE1 inhibitor via two distinct mechanisms, impairing NHEJ DNA damage repair and synergistic forced mitotic entry.

* Corresponding Author:
Eiki Kikuchi, M.D., Ph.D.
Department of Respiratory Medicine, Faculty of Medicine and Graduate School of Medicine, Hokkaido University
North 15, West 7, Kita-ku, Sapporo, 0608638, JAPAN
TEL +81-11-706-5911, FAX +81-11-706-7899
e-mail: eikik@med.hokudai.ac.jp

Abstract

Bromodomain and extraterminal domain (BET) inhibitors are broadly active against distinct types of cancer, including non-small cell lung cancer (NSCLC). Previous studies have addressed the effect of BET-inhibiting drugs on the expression of oncogenes such as *c-Myc*, but DNA damage repair pathways have also been reported to be involved in the efficacy of these drugs. AZD1775, an inhibitor of the G2-M cell cycle checkpoint kinase WEE1, induces DNA damage by promoting premature mitotic entry. Thus, we hypothesized that BET inhibition would increase AZD1775-induced cytotoxicity by impairing DNA damage repair. Here, we demonstrate that combined inhibition of BET and WEE1 synergistically suppresses NSCLC growth both *in vitro* and *in vivo*. Two BET inhibitors, JQ1 and AZD5153, increased and prolonged AZD1775-induced DNA double-strand breaks (DSBs) and concomitantly repressed genes related to non-homologous end joining (NHEJ), including *XRCC4* and *SHLD1*. Furthermore, pharmaceutical inhibition of BET or knockdown of the BET protein BRD4 markedly diminished NHEJ activity, and the BET-inhibitor treatment also repressed myelin transcription factor 1 (MYT1) expression and promoted mitotic entry with subsequent mitotic catastrophe when combined with WEE1 inhibition. Our findings reveal that BET proteins, predominantly BRD4, play an essential role in DSB repair through the NHEJ pathway, and further suggest that combined inhibition of BET and WEE1 could serve as a novel therapeutic strategy for NSCLC.

Introduction

Lung cancer is the leading cause of cancer-related deaths worldwide, and non-small cell lung cancer (NSCLC) accounts for approximately 80% of all lung cancers.[1, 2] Despite the recent development of molecular-targeted drugs and immune checkpoint inhibitors, available therapies have exhibited only limited efficacy in the case of patients with advanced NSCLC, and the survival rates of these patients have remained poor. Consequently, urgent demand exists for developing novel strategies for treating advanced NSCLC.

Bromodomain and extraterminal domain (BET)-family proteins, which include BRD2, BRD3, BRD4, and BRDT, are epigenetic reader proteins that bind to acetylated-lysine residues on histones and promote gene transcription by interacting with positive transcription elongation factor b (P-TEFb) and RNA polymerase II.[3-5] BET inhibitors bind to BET proteins' (predominantly BRD4's) recognition pocket for acetylated-lysine residues and thereby inhibit BET-histone binding and recruitment of transcriptional complexes to genomic loci[6, 7], and the results of preclinical studies have indicated that BET inhibitors are broadly active in different cancer types, including NSCLC.[8-13] Although the effect of BET inhibitors on the expression of oncogenes such as *c-Myc* has been extensively addressed[10, 14], the mechanisms by which BET inhibition produces cytotoxicity remain unknown. However, several recent studies have reported that BRD4 is essential for the repair of DNA double-strand breaks (DSBs), and that BET inhibitors suppress both of the major DSB repair mechanisms, homologous recombination (HR) and non-homologous end joining (NHEJ).[15-18]

The tyrosine kinase WEE1, which is a crucial component of the G2-M cell cycle checkpoint, prevents mitotic entry in response to cellular DNA damage by acting in cooperation with myelin transcription factor 1 (MYT1) kinase. WEE1 and MYT1 kinases inhibit CDK1 activity by phosphorylating CDK1 at Thr14 and Tyr15, which results in the

activation of the G2-M checkpoint and cell cycle arrest.[19] WEE1 also plays a role in regulating DNA replication and maintaining stalled replication forks during the S phase by phosphorylating CDK2.[20, 21] In response to DNA damage, WEE1 and MYT1 kinases inactivate CDK1/CDK2 and thus prevent cells from proceeding through mitosis by maintaining G2 arrest, where adequate time is available for the cells to repair their damaged DNA. WEE1 loss of function induces premature CDK1 activity in the S phase and subsequent unscheduled mitosis coupled with unrepaired DNA damage, which leads to apoptotic death (mitotic catastrophe).[22, 23] In preclinical studies, AZD1775, a selective WEE1 inhibitor, reduced cell viability, increased DNA damage, and induced apoptosis in various cancer cells, but not in normal mammary epithelial cells and fibroblasts.[24] Moreover, a phase I clinical trial of single-agent AZD1775 demonstrated multiple partial responses in patients carrying *BRCA* mutations that could be involved in repairing DNA breaks.[25]

Thus, we hypothesized that BET inhibition would increase WEE1-inhibitor-induced cytotoxicity by impairing DNA damage repair. Here, we present the efficacy and the mechanistic rationale for using combination therapy of WEE1 and BET inhibitors as a potential treatment for NSCLC.

Materials and Methods

Cell culture

Five human NSCLC cell lines, A549, H460, H520, H1299, and H1975, were maintained in RPMI-1640 medium supplemented with 10% FBS and 100 U/mL penicillin-streptomycin in a humidified atmosphere at 37°C with 5% CO_2. The human embryonic kidney cell line 293T was maintained in DMEM supplemented with 10% heat-inactivated FBS under the same conditions.

Cell-proliferation assay

Antitumor activities of each drug applied singly and in combination were analyzed using the MTT cell-proliferation assay, according to the manufacturer's instructions (Thermo Fisher Scientific, Waltham, MA). Synergism between BET inhibitors and AZD1775 was quantified through combination index (CI) analysis, adapted from the median-principle methods of Chou and Talalay[26] using CompuSyn 1.0 software (ComboSyn, Paramus, NJ).

Antibodies and Western blotting

Whole-cell lysates and homogenized snap-frozen tumor nodules were subjected to Western blotting to analyze the expression of various proteins using the specific antibodies listed in Supplementary Table S1.

Immunofluorescence staining

Analysis of mitotic catastrophe were performed as previously reported.[27, 28] For immunofluorescence staining, cells were treated with specified compounds for 24 h. Cells were fixed using 4% paraformaldehyde for 20 min at 4°C and permeablized with PBS containing 0.5% Triton X-100 for 10 min at 4°C. Cells were incubated with Blocking One Histo (Nacalai Tesque, Kyoto, Japan) for 5 min at room temperature to block nonspecific antibody-binding sites. Next, cells were incubated with primary antibody (Supplementary Table S1) at 4°C overnight. They were next incubated with Alexa Flour 488 Goat anti-Rabbit IgG (Thermo Fisher Scientific) for 90 min, followed by DAPI staining. Coverslips were mounted with ProLong Diamond Antifade Mountant reagent (Thermo Fisher Scientific). Fluorescent microscopic analysis was performed using Biorevo BZ-9000 (Keyence, Osaka, Japan).

Quantitative reverse-transcription (RT)-PCR

Expression of each mRNA was determined through quantitative RT-PCR

performed using SYBR Green PCR Master Mix and a StepOnePlus Real-Time PCR System (Applied Biosystems, Foster City, CA). Each sample was amplified in triplicate for quantification of the specified transcript level. Reactions were performed using 1 µg of total RNA. *HPRT1* was amplified as an internal control. The amount of each mRNA is expressed here as arbitrary units, defined as the n-fold difference relative to the control gene *HPRT1* (ΔΔCt method). The primers used are listed in Supplementary Table S2.

siRNA

BRD4 RNA interference was performed using ON-TARGET plus siRNA SMART pool and ON-TARGET plus Non-targeting Control pool (Dharmacon, Lafayette, CO). Knockdown efficiency was measured through Western blotting at 48 h after transfection.

Cell cycle and apoptosis assays

Apoptosis and cell cycle assays were performed using a BD FACSVerse flow cytometer (Becton Dickinson, Franklin Lakes, NJ). For the apoptosis assay, cells were treated with specified compounds or vehicle for 72 h and then stained with Annexin V and Propidium Iodide (PI) using an Annexin V-FITC Apoptosis Detection Kit (Merck Millipore, Burlington, MA) according to the manufacturer's instructions. Cell cycle was analyzed using PI Staining Solution (Becton Dickinson), as per the manufacturer's instructions.

***In vitro* NHEJ DNA repair assay**

NHEJ reporter assay was performed using the chromosomally integrated GFP reporter pimEJ5GFP in H1299 cells (H1299-EJ5), as previously reported[29, 30]; pimEJ5GFP was a gift from Prof. Jeremy Stark (#44026; Addgene, Cambridge, MA). The H1299-EJ5 cells express GFP after successful NHEJ repair of DSBs induced by I-SceI endonuclease. Because DsRed is transfected here together with I-SceI endonuclease using ISceI-GR-RFP

plasmid (#17654; Addgene), the ratio of GFP-positive cells to DsRed-positive cells after I-SceI transfection directly correlates with NHEJ DNA repair activity. At 48 h after I-SceI transfection, GFP and DsRed expression was analyzed using flow cytometer. H1299-EJ5 cells were treated with 0.2 μmol/L JQ1, 0.2 μmol/L AZD5153, or siRNA against BRD4.

Animal experiments

All animal husbandry and experiments were performed using protocols approved by Hokkaido University Animal Experimentation Committee. Tumor cells were prepared by suspending 2 × 10^6 A549 cells in 200 μL of PBS, and the cell suspension was injected subcutaneously into 6–8-week-old female nu/nu immunodeficient nude mice (*n* = 4/group). At 1 week after injection, the mice were randomized and then treated for 5 days each week for 3 weeks with vehicle control, JQ1 (50 mg/kg, I.P.), AZD1775 (20 mg/kg, oral gavage), or the drug combination. After the 3-week treatment, the mice were sacrificed, and tumor nodules were harvested for biochemical studies.

Tumor size and body weight were measured twice weekly for the duration of the study. Tumor size was calculated using this formula: size = length (mm) × width (mm) × width (mm) × 1/2. JQ1 was resuspended in 10% 2-hydroxypropyl-β-cyclodextrin. AZD1775 was dissolved in 0.5% methylcellulose.

Immunohistochemical staining

Dissected xenograft tumors were fixed in 10% formalin for 24 h at room temperature, placed in 70% ethanol, embedded in paraffin, and then sectioned at a thickness of 5 μm. The sections were deparaffinized using xylene and rehydrated using graded concentrations of ethanol. For antigen retrieval, sections were placed in 10 mmol/L citrate buffer, pH 6.0, and heated in a pressure cooker. Next, the sections were immersed in methanol containing 3% H_2O_2 for 10 min to block endogenous peroxidase activity, and

then were incubated with normal goat serum to block nonspecific antibody-binding sites. The sections were reacted consecutively with each primary antibody (Supplementary Table S1), at 4°C overnight. Immunostaining was performed using the biotin-streptavidin immunoperoxidase method, with 3,3-diaminobenzidine used as the chromogen. Hematoxylin solution was used for counterstaining.

Statistical analysis

All data were derived from at least 3 independent experiments and are shown as means ± SD, unless otherwise indicated. Differences between groups were statistically analyzed using the Welch *t* test. $P < 0.05$ was considered statistically significant.

Data availability statement

The data that support the findings of this study are available from the corresponding author upon reasonable request.

Results

Combined application of BET inhibitors and WEE1 inhibitor AZD1775 produces synergistic cytotoxicity in NSCLC cell lines

We first evaluated how combined use of BET inhibitors (JQ1 and AZD5153) and a WEE1 inhibitor (AZD1775) affects the proliferation of 5 NSCLC cell lines with different p53 status (Fig 1A): H1299 (which is p53-null), H1975 (which expresses a mutant p53), H520 (which expresses wild-type but greatly reduced levels of p53), A549, and H460 (the last two of which express wild-type p53). Cell-proliferation assays revealed that combined BET and WEE1 inhibition produced strong synergistic effects (CI: 0.1–0.5) in all 5 cell lines (i.e., the effect was independent of p53 status) (Fig. 1B and 1C; Supplementary Fig. S1A and S1B). Consistently, siRNA-mediated knockdown of the BET protein BRD4 significantly increased

the sensitivity to AZD1775 (Fig. 1D; Supplementary Fig. S2A). Efficient BRD4 knockdown was confirmed through Western blotting (Fig. 1E; Supplementary Fig. S2B). By contrast, the synergistic cytotoxic effect of combined BET and WEE1 inhibition was not observed in non-tumorigenic 293T cells (Supplementary Fig. S2C). Moreover, flow-cytometry results showed that JQ1 induced little apoptosis when applied alone but significantly increased AZD1775-induced apoptosis in A549, H1299, and H1975 cells (Fig. 1F; Supplementary Fig. S3A–C), and Western blotting revealed clear cleavage of PARP and caspase-3 after combined JQ1 and AZD1775 treatment (Supplementary Fig. S3D). Collectively, these results demonstrate that combined inhibition of BET and WEE1 synergistically suppresses cell proliferation by inducing apoptosis in NSCLC cell lines.

BET inhibitors enhance and prolong AZD1775-induced DNA damage

We next assessed the effect of the combined inhibition of BET and WEE1 on DNA damage by measuring γH2AX, a surrogate marker for unrepaired DSBs. In Western blotting analysis, JQ1 or AZD5153 single treatment did not induce γH2AX expression substantially, but combined BET-inhibitor plus AZD1775 treatment markedly increased γH2AX expression relative to that induced by AZD1775 single treatment in all 5 cell lines (Fig. 2A; Supplementary Fig. S4A and S4B). In addition, siRNA-mediated BRD4 knockdown increased γH2AX expression considerably compared to non-target siRNA transfected cells after AZD1775 treatment (Supplementary Fig. S4C). Immunofluorescence staining confirmed that the combined inhibition of BET and WEE1 greatly increased γH2AX-positive cells (Fig. 2B).

To evaluate the impact of BET inhibition on AZD1775-induced DSBs, we examined the temporal changes in γH2AX expression (Fig. 2C). AZD1775 upregulated γH2AX expression, which peaked at 4 h after the end of the drug exposure and declined thereafter; however, JQ1 treatment persistently impaired the reversal of AZD1775-induced γH2AX

expression (Fig. 2D), and thus, the γH2AX level was significantly elevated at 8 h after the end of AZD1775 exposure (Fig. 2E). These results demonstrate that BET inhibition disrupts the repair of AZD1775-induced DSBs.

BET inhibitors repress the expression of NHEJ-related genes

We reasoned that BET proteins mediate the transcriptional regulation of DSB repair genes. Therefore, we examined the mRNA expression of DSB repair-related genes after BET inhibition. After treatment with JQ1 or AZD5153, the expression of HR pathway-related genes was nearly unchanged (Supplementary Fig. S5A and S5B), but a considerable reduction was observed in the expression of NHEJ pathway-related genes, including *SHLD1*, *SHLD3*, *XRCC4*, *SASS6*, and *TP53BP1* (Fig. 3A; Supplementary Fig. S5C and S6A–D). Western blotting results confirmed that the BET inhibitors decreased the expression of proteins involved in the NHEJ pathway (Fig. 3B; Supplementary Fig. S5D).

BRD4 inhibition diminishes NHEJ activity

To test whether BET inhibition hampers NHEJ, we used an engineered H1299-EJ5 NHEJ reporter cell line; in these cells, GFP is expressed after successful NHEJ repair of DSBs induced by I-SceI endonuclease. The ratio of GFP-positive cells was significantly decreased after treatment with JQ1 (Fig. 3C; Supplementary Fig. S7) or AZD5153 (Fig. 3D), and NHEJ activity was also significantly impaired after siRNA-mediated knockdown of BRD4 (Fig. 3E). These results indicate that BET inhibition, predominantly BRD4 inhibition, critically affects the NHEJ pathway.

BET inhibition represses MYT1 and synergizes with WEE1 inhibition to promote mitotic entry and mitotic catastrophe

We evaluated how the combined inhibitor treatment affects cell cycle progression.

JQ1 treatment has been shown to induce G1 arrest.[9, 31, 32] Unexpectedly, in 2/3 cell lines tested, JQ1 treatment in combination with AZD1775 resulted in a significant increase in the percentage of cells in G2-M phase as compared with the percentages after single treatments (Fig. 4A–C). Furthermore, the combined treatment increased the level of phosphorylated histone H3 (pHH3) relative to that after each single treatment in all 5 cell lines (Fig. 4D; Supplementary Fig. S8A and S8B). Obvious G1 arrest was not observed in the cells after JQ1 treatment. Quantitative RT-PCR analysis of G2-M checkpoint-related genes revealed that BET inhibitors significantly reduced the expression of *MYT1* (Fig. 4E; Supplementary Fig. S9A and S9B), and Western blotting results confirmed that the BET inhibitors decreased MYT1 expression (Fig. 4F; Supplementary Fig. S9C). Because MYT1 acts in concert with WEE1 to restrain G2-M transition as a crucial component of the G2-M cell cycle checkpoint, it is reasonable that BET inhibition-induced MYT1 suppression could promote mitotic entry when WEE1 is simultaneously inhibited.

Next, we examined the effects of the combined inhibition of BET and WEE1 on mitotic catastrophe using immunofluorescence staining. Cells that displayed signs of aberrant nuclei, such as micronuclei, multi-lobular nuclei, or fragment nuclei, were regarded as cells undergoing mitotic catastrophe as previously reported (Fig. 5A).[28] The combined JQ1 and AZD1775 treatment considerably increased mitotic catastrophe relative to that after each single treatment (Fig. 5B). Furthermore, abnormal mitosis with unaligned, dispersed chromosomes and disorganized multipolar spindles were observed after the combined treatment (Fig. 5C). These results suggest that BET inhibition suppresses MYT1 expression and synergizes with WEE1 inhibition to promote forced mitotic entry and subsequent mitotic catastrophe.

Combined inhibition of BET and WEE1 synergistically reduces tumor growth *in vivo*

Lastly, we examined whether the combined inhibition of BET and WEE1 also

exhibits synergism in an *in vivo* setting. JQ1 and AZD1775 were administered either as single agents or in combination to A549 tumor-bearing mice. The single-drug treatment and the combination therapy of JQ1 and AZD1775 were both well tolerated, and no significant body weight loss was observed in the treated mice (Supplementary Fig. S10). After 3 weeks of administration, the combination therapy significantly reduced tumor growth as compared to each single treatment (Fig. 6A). In accord with the *in vitro* findings, pharmacodynamics analysis revealed that the combination therapy significantly increased γH2AX and pHH3 levels in xenograft tumor nodules, as shown by the results of immunohistochemical staining (Fig. 6B–D) and Western blotting (Fig. 6E). The Western blotting results showed that MYT1 expression in the xenograft tumors was also suppressed after the combined treatment (Fig. 6E).

Discussion

We have shown here that BET inhibition synergizes with WEE1 inhibition to kill NSCLC cells in both *in vitro* and *in vivo* settings. We found that the mechanisms underlying this synergistic cytotoxicity include BET inhibition-induced impairment of NHEJ DNA damage repair and synergistic forced mitotic entry.

Recently, BET inhibitors have been reported to hamper DNA damage repair through several distinct mechanisms. Li *et al.* reported that BRD4 participated in NHEJ DNA repair by regulating NHEJ DNA repair genes and interacting with NHEJ DNA repair proteins.[17] Wang *et al.* discovered a BRD-like module in the catalytic subunit of DNA-dependent protein kinase (DNA-PKcs-BRD) to which JQ1 could bind, and further showed that JQ1 hampered NHEJ DNA repair by impairing DNA-PKcs activity.[33] Sun *et al.* reported that BRD4 inhibition blocked DNA end resection and HR through downregulation of CtIP (C-terminal binding protein interacting protein).[18] In this study, we observed that BET inhibition repressed the expression of NHEJ-related genes. The genes repressed by BET

inhibitors varied slightly among the tested cell lines but included *SHLD1*, *SHLD3*, *XRCC4*, *SASS6*, and *TP53BP1*. Notably, BET inhibitors downregulated *XRCC4* by ~70% in all 3 cell lines and *SHLD1* by ~90% in A549 and H1975 cells. Recently, SHLD1 was reported to be a component of the shieldin complex, which is a key regulator of NHEJ[30, 34, 35]; the shieldin complex functions downstream of TP53BP1 and suppresses DNA end resection and promotes NHEJ. Our study here indicates that BET inhibitors could suppress NHEJ-related genes and thereby impair NHEJ.

JQ1 appears to decrease more NHEJ activity compared with siBRD4 or AZD5153 (Fig. 3C-E). Recent studies have identified a lot of human BRD proteins directly responding to DNA damage.[36] In addition, Li *et al*. reported that c-Myc interacted directly with Ku70 protein and inhibited DNA repair, and that loss of c-Myc recovered the impairment of DSB repair.[37] Thus, indirect effects of BET inhibitors could impact NHEJ activity, and the intensity of the NHEJ impairment may depend on the cellular context.

The choice between HR and NHEJ depends primarily on the cell cycle stage. HR is inhibited during the G1 phase when sister chromatids are not available, whereas NHEJ is active throughout the cell cycle phase.[38] In the mitotic phase, little repair of DNA damage occurs, but the damage is detected and marked for repair after mitotic exit, mainly by NHEJ in the G1 phase.[39] WEE1 inhibition promotes the mitotic entry of DNA-damaged cells, and the damaged cells could be repaired by NHEJ in the G1 phase. Thus, BET inhibition-induced NHEJ impairment could enhance the efficacy of WEE1 inhibition.

BET inhibitors have been widely reported to sensitize cancer cells to several genotoxic agents, such as PARP inhibitors[15, 18], platinums[40], and topoisomerase inhibitors.[41] These agents induce S-phase dependent DNA damage, which is predominantly repaired by HR. In contrast, as WEE1 inhibitors make mitotic cells have damaged DNA, HR may not repair the DNA damage induced by WEE1 inhibitors. Our data highlight the impact of BET inhibitors on NHEJ by means of combination with WEE1 inhibition.

Several papers also have reported that BET inhibitors synergize with cell cycle checkpoint modulators, such as CDK inhibitors[42] or ATR inhibitors.[31, 43] Zhang et al. reported that BRD4 inhibitor synergized with an ATR inhibitor through reducing the phosphorylation of CHK1.[43] CHK1 inhibitors would also synergize with BET inhibitors theoretically, as CHK1 inhibitors could drive mitotic entry. However, the effects of these combinations on DNA repair or cell cycle remain uncertain and will require further investigations.

AZD1775 has been widely found to show higher cytotoxicity in p53-deleted or -mutated cells than in wild-type p53-expressing cells.[44-46] These results potentially support the notion that cancers lacking functional p53, a key component of the G1-S checkpoint, exhibit increased reliance on the G2-M checkpoint, and that p53-deficient cells show enhanced susceptibility to abrogation of the G2-M checkpoint following WEE1 inhibition. However, other studies have shown that the efficacy is independent of p53 status.[47, 48] In this study, the synergistic toxicity produced by combined inhibition of BET and WEE1 was found to be independent of the p53 status.

We showed that BET inhibition also represses MYT1 expression, and that the combined inhibition of BET and WEE1 increased the level of the mitosis-specific marker pHH3. WEE1 and MYT1 act in concert to function as a gatekeeper of G2-M checkpoint arrest. Guertin *et al.* reported that AZD1775-sensitive cell lines tend to exhibit diminished MYT1 expression, and that MYT1 knockdown enhances the sensitivity of cancer cells to AZD1775 coupled with an increase in DNA damage.[48] Our study here is the first to show that BET inhibitors act as suppressors of MYT1 expression and sensitize cells to a WEE1 inhibitor.

Considering clinical utility of the combined inhibition of BET and WEE1, it will be necessary to assess if concurrent or sequential use of these inhibitors offers more advantages. We showed that AZD1775 pretreatment and sequential JQ1 administration generated prolonged DSB. On the other hand, the previous preclinical study has shown that

JQ1 pretreatment enhanced irradiation-induced DNA damage in NSCLC cells.[49] Further investigations will be needed to clarify the efficacy of the sequential treatment of BET and WEE1 inhibitors.

Currently, multiple BET inhibitors are in various stages of clinical development. The results of a phase Ib trial of birabresib, a selective BET inhibitor, in patients with advanced solid tumors, including 10 NSCLC patients, indicated that birabresib single treatment exhibited a favorable safety profile but produced limited cytotoxic effects[50]; given these results, single treatment with BET inhibitors might be insufficient, and combination treatment with other agents could be crucial in the case of patients with solid tumors. For castration-resistant prostate cancer, trials of combination treatment with BET inhibitors and androgen receptor blockers are ongoing (ClinicalTrials.gov identifiers: NCT02607228 and NCT02711956). The results of phase I trials of AZD1775 as single treatment and in combination with existing systemic chemotherapy in patients with solid tumors indicated that AZD1775 was safe and tolerable both as a single agent and in combination with chemotherapy.[25, 51] Confirmed partial responses were observed after single AZD1775 treatment in 2/25 patients with refractory solid tumors.[25] Multiple phase II trials of AZD1775 in single or combination treatment for solid tumors are ongoing.

In conclusion, we demonstrated that combined inhibition of BET and WEE1 induced strong synergistic cytotoxicity in NSCLC cells both *in vitro* and *in vivo*. The effect can be attributed to two findings: (i) BET inhibition increases and prolongs WEE1-inhibitor-induced DSBs by impairing DSB repair through the NHEJ pathway; and (ii) BET inhibition represses MYT1 expression and abrogates G2-M checkpoint in concert with WEE1 inhibition and thereby leads to mitotic catastrophe. Our preclinical results can help in optimizing future use of BET-inhibitor and WEE1-inhibitor treatment for NSCLC.

Financial Support

This research received no specific grant from any funding agency in the public, commercial, or not-for-profit sectors.

Conflict of interest statement

There is no conflict of interest to declare.

References

1. Siegel RL, Miller KD, Jemal A. Cancer statistics, 2018. CA Cancer J Clin 2018;68: 7-30.

2. Rothschild SI. Targeted therapies in non-small cell lung cancer-beyond EGFR and ALK. Cancers 2015;7: 930-949.

3. Dey A, Chitsaz F, Abbasi A, Misteli T, Ozato K. The double bromodomain protein Brd4 binds to acetylated chromatin during interphase and mitosis. Proc Natl Acad Sci U S A 2003;100: 8758-8763.

4. Shi J, Vakoc CR. The mechanisms behind the therapeutic activity of BET bromodomain inhibition. Mol Cell 2014;54: 728-736.

5. Yang Z, Yik JH, Chen R, He N, Jang MK, Ozato K, Zhou Q. Recruitment of P-TEFb for stimulation of transcriptional elongation by the bromodomain protein Brd4. Mol Cell 2005;19: 535-545.

6. Rhyasen GW, Hattersley MM, Yao Y, Dulak A, Wang W, Petteruti P, Dale IL, Boiko S, Cheung T, Zhang J, Wen S, Castriotta L, Lawson D, Collins M, Bao L, Ahdesmaki MJ, Walker G, O'Connor G, Yeh TC, Rabow AA, Dry JR, Reimer C, Lyne P, Mills GB, Fawell SE, Waring MJ, Zinda M, Clark E, Chen H. AZD5153: a novel bivalent BET bromodomain inhibitor highly active against hematologic malignancies. Mol Cancer Ther 2016;15: 2563-2574.

7. Filippakopoulos P, Qi J, Picaud S, Shen Y, Smith WB, Fedorov O, Morse EM, Keates T, Hickman TT, Felletar I, Philpott M, Munro S, McKeown MR, Wang Y, Christie AL, West N, Cameron MJ, Schwartz B, Heightman TD, La Thangue N, French CA, Wiest O, Kung AL, Knapp S, Bradner JE. Selective inhibition of BET bromodomains. Nature 2010;468: 1067-1073.

8. Cheng Z, Gong Y, Ma Y, Lu K, Lu X, Pierce LA, Thompson RC, Muller S, Knapp S, Wang J. Inhibition of BET bromodomain targets genetically diverse glioblastoma. Clin

Cancer Res 2013;19: 1748-1759.

9. Lockwood WW, Zejnullahu K, Bradner JE, Varmus H. Sensitivity of human lung adenocarcinoma cell lines to targeted inhibition of BET epigenetic signaling proteins. Proc Natl Acad Sci U S A 2012;109: 19408-19413.

10. Mertz JA, Conery AR, Bryant BM, Sandy P, Balasubramanian S, Mele DA, Bergeron L, Sims RJ, 3rd. Targeting MYC dependence in cancer by inhibiting BET bromodomains. Proc Natl Acad Sci U S A 2011;108: 16669-16674.

11. Shimamura T, Chen Z, Soucheray M, Carretero J, Kikuchi E, Tchaicha JH, Gao Y, Cheng KA, Cohoon TJ, Qi J, Akbay E, Kimmelman AC, Kung AL, Bradner JE, Wong KK. Efficacy of BET bromodomain inhibition in Kras-mutant non-small cell lung cancer. Clin Cancer Res 2013;19: 6183-6192.

12. Wyce A, Degenhardt Y, Bai Y, Le B, Korenchuk S, Crouthame MC, McHugh CF, Vessella R, Creasy CL, Tummino PJ, Barbash O. Inhibition of BET bromodomain proteins as a therapeutic approach in prostate cancer. Oncotarget 2013;4: 2419-2429.

13. Zhu X, Enomoto K, Zhao L, Zhu YJ, Willingham MC, Meltzer P, Qi J, Cheng SY. Bromodomain and extraterminal protein inhibitor JQ1 suppresses thyroid tumor growth in a mouse model. Clin Cancer Res 2017;23: 430-440.

14. Delmore JE, Issa GC, Lemieux ME, Rahl PB, Shi J, Jacobs HM, Kastritis E, Gilpatrick T, Paranal RM, Qi J, Chesi M, Schinzel AC, McKeown MR, Heffernan TP, Vakoc CR, Bergsagel PL, Ghobrial IM, Richardson PG, Young RA, Hahn WC, Anderson KC, Kung AL, Bradner JE, Mitsiades CS. BET bromodomain inhibition as a therapeutic strategy to target c-Myc. Cell 2011;146: 904-917.

15. Yang L, Zhang Y, Shan W, Hu Z, Yuan J, Pi J, Wang Y, Fan L, Tang Z, Li C, Hu X, Tanyi JL, Fan Y, Huang Q, Montone K, Dang CV, Zhang L. Repression of BET activity sensitizes homologous recombination-proficient cancers to PARP inhibition. Sci Transl Med 2017;9:eaal1645.

16. Stanlie A, Yousif AS, Akiyama H, Honjo T, Begum NA. Chromatin reader Brd4 functions in Ig class switching as a repair complex adaptor of nonhomologous end-joining. Mol Cell 2014;55: 97-110.

17. Li X, Baek G, Ramanand SG, Sharp A, Gao Y, Yuan W, Welti J, Rodrigues DN, Dolling D, Figueiredo I, Sumanasuriya S, Crespo M, Aslam A, Li R, Yin Y, Mukherjee B, Kanchwala M, Hughes AM, Halsey WS, Chiang CM, Xing C, Raj GV, Burma S, de Bono J, Mani RS. BRD4 promotes DNA repair and mediates the formation of TMPRSS2-ERG gene rearrangements in prostate cancer. Cell Rep 2018;22: 796-808.

18. Sun C, Yin J, Fang Y, Chen J, Jeong KJ, Chen X, Vellano CP, Ju Z, Zhao W, Zhang D, Lu Y, Meric-Bernstam F, Yap TA, Hattersley M, O'Connor MJ, Chen H, Fawell S, Lin SY, Peng G, Mills GB. BRD4 inhibition is synthetic lethal with PARP inhibitors through the induction of homologous recombination deficiency. Cancer Cell 2018;33: 401-416.e8.

19. O'Connell MJ, Raleigh JM, Verkade HM, Nurse P. Chk1 is a wee1 kinase in the G2 DNA damage checkpoint inhibiting cdc2 by Y15 phosphorylation. EMBO J 1997;16: 545-554.

20. Vriend LE, De Witt Hamer PC, Van Noorden CJ, Würdinger T. WEE1 inhibition and genomic instability in cancer. Biochim Biophys Acta 2013;1836: 227-235.

21. Do K, Doroshow JH, Kummar S. Wee1 kinase as a target for cancer therapy. Cell Cycle 2013;12: 3159-3164.

22. Matheson CJ, Backos DS, Reigan P. Targeting WEE1 kinase in cancer. Trends Pharmacol Sci 2016;37: 872-881.

23. Beck H, Nähse V, Larsen MS, Groth P, Clancy T, Lees M, Jorgensen M, Helleday T, Syljuasen RG, Sorensen CS. Regulators of cyclin-dependent kinases are crucial for maintaining genome integrity in S phase. J Cell Biol 2010;188: 629-638.

24. Murrow LM, Garimella SV, Jones TL, Caplen NJ, Lipkowitz S. Identification of WEE1 as a potential molecular target in cancer cells by RNAi screening of the human

tyrosine kinome. Breast Cancer Res Treat 2010;122: 347-357.

25. Do K, Wilsker D, Ji J, Zlott J, Freshwater T, Kinders RJ, Collins J, Chen AP, Doroshow JH, Kummar S. Phase I study of single-agent AZD1775 (MK-1775), a Wee1 kinase inhibitor, in patients with refractory solid tumors. J Clin Oncol 2015;33: 3409-3415.

26. Chou TC. Drug combination studies and their synergy quantification using the Chou-Talalay method. Cancer Res 2010;70: 440-446.

27. Suzuki M, Yamamori T, Yasui H, Inanami O. Effect of MPS1 inhibition on genotoxic stress responses in murine tumour cells. *Anticancer Res* 2016;36: 2783-2792.

28. Suzuki M, Yamamori T, Bo T, Sakai Y, Inanami O. MK-8776, a novel Chk1 inhibitor, exhibits an improved radiosensitizing effect compared to UCN-01 by exacerbating radiation-induced aberrant mitosis. *Transl Oncol* 2017;10: 491-500.

29. Bennardo N, Cheng A, Huang N, Stark JM. Alternative-NHEJ is a mechanistically distinct pathway of mammalian chromosome break repair. PLoS Genet 2008;4: e1000110.

30. Gupta R, Somyajit K, Narita T, Maskey E, Stanlie A, Kremer M, Typas D, Lammers M, Mailand N, Nussenzweig A, Lukas J, Choudhary C. DNA repair network analysis reveals shieldin as a key regulator of NHEJ and PARP inhibitor sensitivity. Cell 2018;173: 972-988.e23.

31. Muralidharan SV, Einarsdottir BO, Bhadury J, Lindberg MF, Wu J, Campeau E, Bagge RO, Stierner U, Ny L, Nilsson LM, Nilsson JA. BET bromodomain inhibitors synergize with ATR inhibitors in melanoma. Cell Death Dis 2017;8: e2982.

32. Wu X, Liu D, Tao D, Xiang W, Xiao X, Wang M, Wang L, Luo G, Li Y, Zeng F, Jiang G. BRD4 Regulates EZH2 transcription through upregulation of C-MYC and represents a novel therapeutic target in bladder cancer. Mol Cancer Ther 2016;15: 1029-1042.

33. Wang L, Xie L, Ramachandran S, Lee Y, Yan Z, Zhou L, Krajewski K, Liu F,

512 Zhu C, Chen DJ, Strahl BD, Jin J, Dokholyan NV, Chen X. Non-canonical bromodomain
513 within DNA-PKcs promotes DNA damage response and radioresistance through
514 recognizing an IR-induced acetyl-lysine on H2AX. Chem Biol 2015;22: 849-861.
515 34. Ghezraoui H, Oliveira C, Becker JR, Bilham K, Moralli D, Anzilotti C, Fischer R,
516 Deobagkar-Lele M, Sanchiz-Calvo M, Fueyo-Marcos E, Bonham S, Kessler BM,
517 Rottenberg S, Cornall RJ, Green CM, Chapman JR. 53BP1 cooperation with the REV7-
518 shieldin complex underpins DNA structure-specific NHEJ. Nature 2018;560: 122-127.
519 35. Noordermeer SM, Adam S, Setiaputra D, Barazas M, Pettitt SJ, Ling AK,
520 Olivieri M, Alvarez-Quilon A, Moatti N, Zimmermann M, Annunziato S, Krastev DB, Song F,
521 Brandsma I, Frankum J, Brough R, Sherker A, Landry S, Szilard RK, Munro MM, McEwan
522 A, Goullet de Rugy T, Lin ZY, Hart T, Moffat J, Gingras AC, Martin A, van Attikum H, Jonkers
523 J, Lord CJ, Rottenberg S, Durocher D. The shieldin complex mediates 53BP1-dependent
524 DNA repair. Nature 2018;560: 117-121.
525 36. Gong F, Chiu LY, Miller KM. Acetylation reader proteins: linking acetylation
526 signaling to genome maintenance and cancer. *PLoS genetics* 2016;12: e1006272.
527 37. Li Z, Owonikoko TK, Sun SY, Ramalingam SS, Doetsch PW, Xiao ZQ, Khuri
528 FR, Curran WJ, Deng X. C-Myc suppression of DNA double-strand break repair. *Neoplasia*
529 2012;14: 1190-1202.
530 38. van Gent DC, Kanaar R. Exploiting DNA repair defects for novel cancer
531 therapies. Mol Biol Cell 2016;27: 2145-2148.
532 39. Heijink AM, Krajewska M, van Vugt MA. The DNA damage response during
533 mitosis. Mutat Res 2013;750: 45-55.
534 40. Zanellato I, Colangelo D, Osella D. JQ1, a BET Inhibitor, synergizes with
535 cisplatin and induces apoptosis in highly chemoresistant malignant pleural mesothelioma
536 cells. *Curr Cancer Drug Targets* 2018;18: 816-828.
537 41. Kaur G, Reinhart RA, Monks A, Evans D, Morris J, Polley E, Teicher BA.

538 Bromodomain and hedgehog pathway targets in small cell lung cancer. *Cancer Lett*
539 2016;371: 225-239.
540 42. Tomska K, Kurilov R, Lee KS, Hullein J, Lukas M, Sellner L, Walther T, Wagner
541 L, Oles M, Brors B, Huber W, Zenz T. Drug-based perturbation screen uncovers synergistic
542 drug combinations in Burkitt lymphoma. *Sci Rep* 2018;8: 12046.
543 43. Zhang J, Dulak AM, Hattersley MM, Willis BS, Nikkila J, Wang A, Lau A, Reimer
544 C, Zinda M, Fawell SE, Mills GB, Chen H. BRD4 facilitates replication stress-induced DNA
545 damage response. *Oncogene* 2018;37: 3763-3777.
546 44. Hirai H, Iwasawa Y, Okada M, Arai T, Nishibata T, Kobayashi M, Kimura T,
547 Kaneko N, Ohtani J, Yamanaka K, Itadani H, Takahashi-Suzuki I, Fukasawa K, Oki H,
548 Nambu T, Jiang J, Sakai T, Arakawa H, Sakamoto T, Sagara T, Yoshizumi T, Mizuarai S,
549 Kotani H. Small-molecule inhibition of Wee1 kinase by MK-1775 selectively sensitizes p53-
550 deficient tumor cells to DNA-damaging agents. Mol Cancer Ther 2009;8: 2992-3000.
551 45. Rajeshkumar NV, De Oliveira E, Ottenhof N, Watters J, Brooks D, Demuth T,
552 Shumway SD, Mizuarai S, Hirai H, Maitra A, Hidalgo M. MK-1775, a potent Wee1 inhibitor,
553 synergizes with gemcitabine to achieve tumor regressions, selectively in p53-deficient
554 pancreatic cancer xenografts. Clin Cancer Res 2011;17: 2799-2806.
555 46. Bridges KA, Hirai H, Buser CA, Brooks C, Liu H, Buchholz TA, Molkentine JM,
556 Mason KA, Meyn RE. MK-1775, a novel Wee1 kinase inhibitor, radiosensitizes p53-
557 defective human tumor cells. Clin Cancer Res 2011;17: 5638-5648.
558 47. Van Linden AA, Baturin D, Ford JB, Fosmire SP, Gardner L, Korch C, Reigan
559 P, Porter CC. Inhibition of Wee1 sensitizes cancer cells to antimetabolite chemotherapeutics
560 in vitro and in vivo, independent of p53 functionality. Mol Cancer Ther 2013;12: 2675-2684.
561 48. Guertin AD, Li J, Liu Y, Hurd MS, Schuller AG, Long B, Hirsch HA, Feldman I,
562 Benita Y, Toniatti C, Zawel L, Fawell SE, Gilliland DG, Shumway SD. Preclinical evaluation
563 of the WEE1 inhibitor MK-1775 as single-agent anticancer therapy. Mol Cancer Ther

2013;12: 1442-1452.

49. Wang J, Wang Y, Mei H, Yin Z, Geng Y, Zhang T, Wu G, Lin Z. The BET bromodomain inhibitor JQ1 radiosensitizes non-small cell lung cancer cells by upregulating p21. *Cancer Lett* 2017;391: 141-151.

50. Lewin J, Soria JC, Stathis A, Delord JP, Peters S, Awada A, Aftimos PG, Bekradda M, Rezai K, Zeng Z, Hussain A, Perez S, Siu LL, Massard C. Phase Ib trial with birabresib, a small-molecule inhibitor of bromodomain and extraterminal proteins, in patients with selected advanced solid tumors. J Clin Oncol 2018: JCO2018782292.

51. Leijen S, van Geel RM, Pavlick AC, Tibes R, Rosen L, Razak AR, Lam R, Demuth T, Rose S, Lee MA, Freshwater T, Shumway S, Liang LW, Oza AM, Schellens JH, Shapiro GI. Phase I study evaluating WEE1 inhibitor AZD1775 as monotherapy and in combination with gemcitabine, cisplatin, or carboplatin in patients with advanced solid tumors. J Clin Oncol 2016;34: 4371-4380.

Figure Legends

Figure 1.

Combined inhibition of BET and WEE1 produces synergistic cytotoxicity in NSCLC cell lines. (**A**) Western blotting analysis of p53 in NSCLC cell lines. Combination index plots for JQ1 and AZD1775 (**B**) or AZD5153 and AZD1775 (**C**); Fraction affected and combination index were calculated using MTT cell-proliferation assay. (**D**) Dose-response curves of the viability of A549 cells transfected BRD4 siRNA or non-target (NT) siRNA followed by AZD1775 administration. Circles: mean values (n = 4/group); bars: SD. *P < 0.05, Welch t test. (**E**) Western blotting results showing the efficiency of BRD4 knockdown through RNA interference. (**F**) Bar charts showing percentages of apoptotic cells among A549 cells after 72 h treatment with vehicle or indicated compounds. Apoptotic-cell percentages were determined using flow cytometry and Annexin V/PI double staining. Boxes: mean values (n = 3/group); error bars: SD. *P < 0.05, Welch t test.

Figure 2.

BET inhibitors enhance and prolong AZD1775-induced DNA damage. (**A**) Western blotting analysis of γH2AX in cells treated with vehicle or indicated compounds for 24 h. (**B**) Immunofluorescence images for γH2AX in A549 cells treated with vehicle or indicated compounds for 24 h (at 0.2 μmol/L). Scale bars in main images: 10 μm. Bar chart: percentages of γH2AX positive cells. Boxes: mean values (n = 3/group); error bars: SD. *P < 0.05, Welch t test. Positive and total tumor cells were counted in 5 high-power fields in the case of each sample (n = 3/group). (**C**) Experimental scheme for evaluating the temporal impact of JQ1 on γH2AX protein expression. A549 cells were treated with 1.0 μmol/L AZD1775 for 24 h to induce γH2AX, after which the cells were washed and incubated with 1.0 μmol/L JQ1 or vehicle for the indicated periods and harvested for Western blotting. (**D**) Western blotting results showing temporal changes in γH2AX expression. Bar chart: γH2AX

levels normalized relative to those of actin; γH2AX expression level at 0 h was arbitrarily designated as 1. (**E**) Western blotting results showing γH2AX level at 8 h after the end of AZD1775 exposure. Bar chart: γH2AX expression levels normalized relative to those of actin; mean expression level of vehicle group was arbitrarily designated as 1. Boxes: mean values; error bars: SD. *P < 0.05, Welch t test.

Figure 3.

BET inhibition represses the expression of NHEJ pathway-related genes and diminishes NHEJ activity. Quantitative RT-PCR (**A**) and Western blotting (**B**) analyses of NHEJ pathway-related genes and proteins in A549 cells treated for 24 h with 1.0 μmol/L indicated compounds or vehicle. Boxes: mean values (n = 3/group); error bars: SD. Bar charts showing NHEJ efficiency quantified using EJ5-GFP reporter after treatment with 0.2 μmol/L JQ1 (**C**), 0.2 μmol/L AZD5153 (**D**), or siRNA against BRD4 (**E**). Mean value of vehicle group was arbitrarily designated as 1. Boxes: mean values (n = 3/group); error bars: SD. *P < 0.05, Welch t test.

Figure 4.

BET inhibition represses MYT1 and synergizes with WEE1 inhibition to promote mitotic entry. Cell cycle profiles of A549 (**A**), H1299 (**B**), and H1975 (**C**) cells after 24 h treatment with indicated compounds (at 1.0 μmol/L) or vehicle. Boxes: mean values (n = 3/group); error bars: SD. *P < 0.05, Welch t test. (**D**) Western blotting analysis of phosphorylated histone H3 (pHH3) in cells treated with indicated compounds or vehicle for 24 h. (**E**) Quantitative RT-PCR analysis of G2-M checkpoint-related genes in A549 cells treated with 1.0 μmol/L JQ1 or vehicle for 24 h. Boxes: mean values (n = 3/group); error bars: SD. (**F**) Western blotting analysis of MYT1 in cells treated with JQ1 or vehicle for 24 h.

Figure 5.

Combined inhibition of BET and WEE1 promotes mitotic catastrophe. (**A**) Representative images of A549 cells possessing features of mitotic catastrophe, such as micronuclei, fragmented nuclei, and multilobular nuclei. Scale bars represent 10 μm. (**B**) Bar charts showing percentages of mitotic catastrophe in A549 cells after 24 h treatment with indicated compounds (at 0.2 μmol/L) or vehicle. Boxes: mean values (n = 3/group); error bars: SD. *P < 0.05, Welch t test. Positive and total tumor cells were counted in 5 high-power fields in the case of each sample (n = 3/group). (**C**) Representative images of abnormal mitotic cells among A549 cells after 24 h combination treatment (at 0.2 μmol/L). Scale bars represent 10 μm.

Figure 6.

Combined inhibition of BET and WEE1 suppresses tumor growth in a mouse xenograft model of NSCLC. (**A**) Growth curves of tumors in nu/nu mice implanted with A549 cells and treated with JQ1 (50 mg/kg), AZD1775 (20 mg/kg), or their combination. Circles: mean volumes (n = 4/group); bars: SD. (**B**) Representative low- and high-magnification images of xenograft tumors subject to hematoxylin and eosin (H&E) staining and immunohistochemical staining for γH2AX and pHH3. Scale bars in main images: 50 μm. (**C**, **D**) Percentages of γH2AX-positive (**C**) and pHH3-positive (**D**) cells in mouse xenograft tumors. Positive and total tumor cells were counted in 5 high-power fields in the case of each sample (n = 4/group). Horizontal lines: means ± SD. *P < 0.05, Welch t test. (**E**) Western blotting analysis of MYT1, γH2AX, and pHH3 in mouse xenograft tumors.

Figure 1.

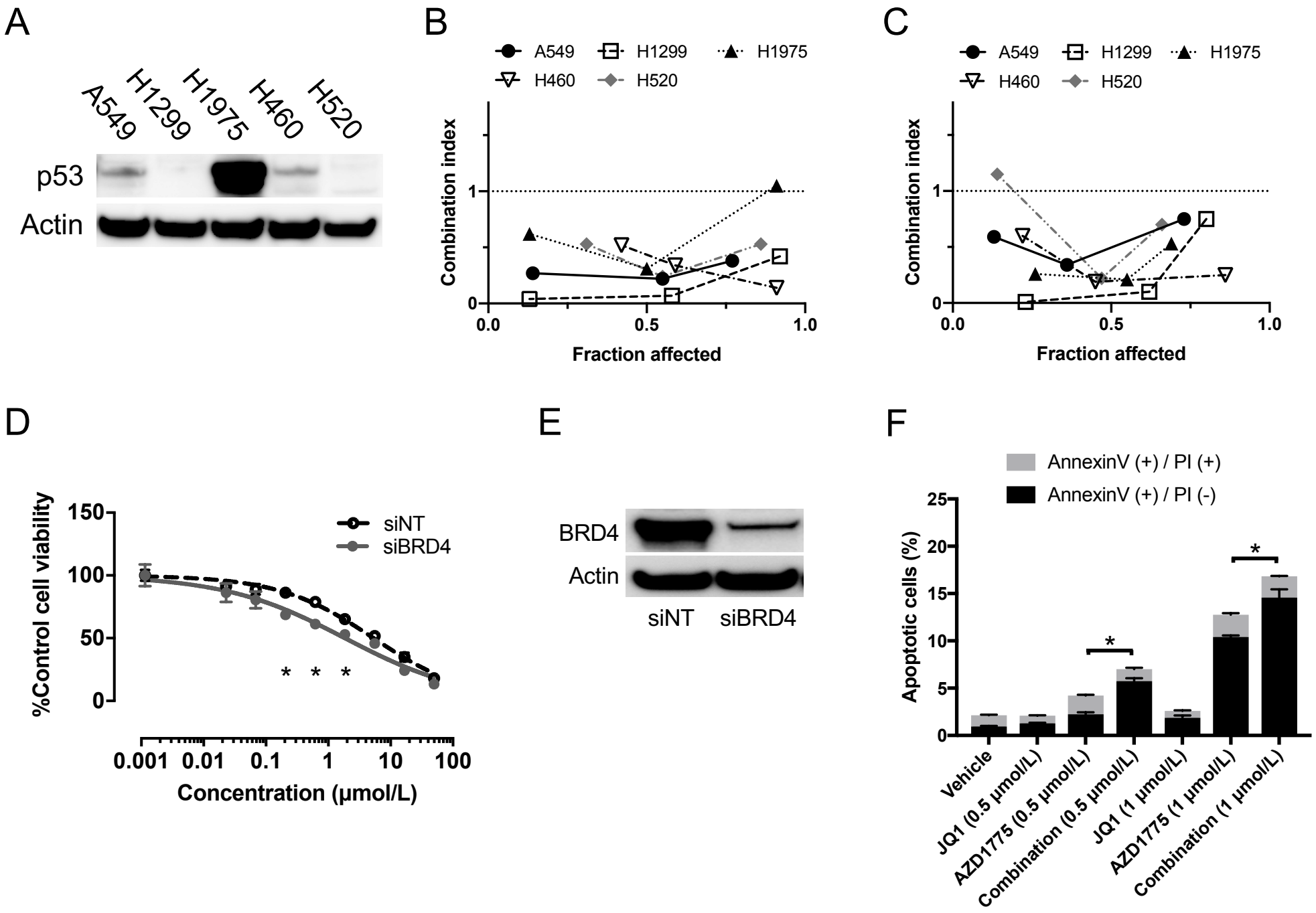
A
A549
H1299
H1975
H460
H520
p53
Actin
B
A549
H1299
H1975
H460
H520
Combination index
1
0
0.0
0.5
1.0
Fraction affected
C
A549
H1299
H1975
H460
H520
Combination index
1
0
0.0
0.5
1.0
Fraction affected
D
%Control cell viability
150
100
50
0
siNT
siBRD4
* * *
0.001 0.01 0.1 1 10 100
Concentration (μmol/L)
E
BRD4
Actin
siNT siBRD4
F
AnnexinV (+) / PI (+)
AnnexinV (+) / PI (-)
Apoptotic cells (%)
25
20
15
10
5
0
*
*
Vehicle
JQ1 (0.5 μmol/L)
AZD1775 (0.5 μmol/L)
Combination (0.5 μmol/L)
JQ1 (1 μmol/L)
AZD1775 (1 μmol/L)
Combination (1 μmol/L)

Figure 2.

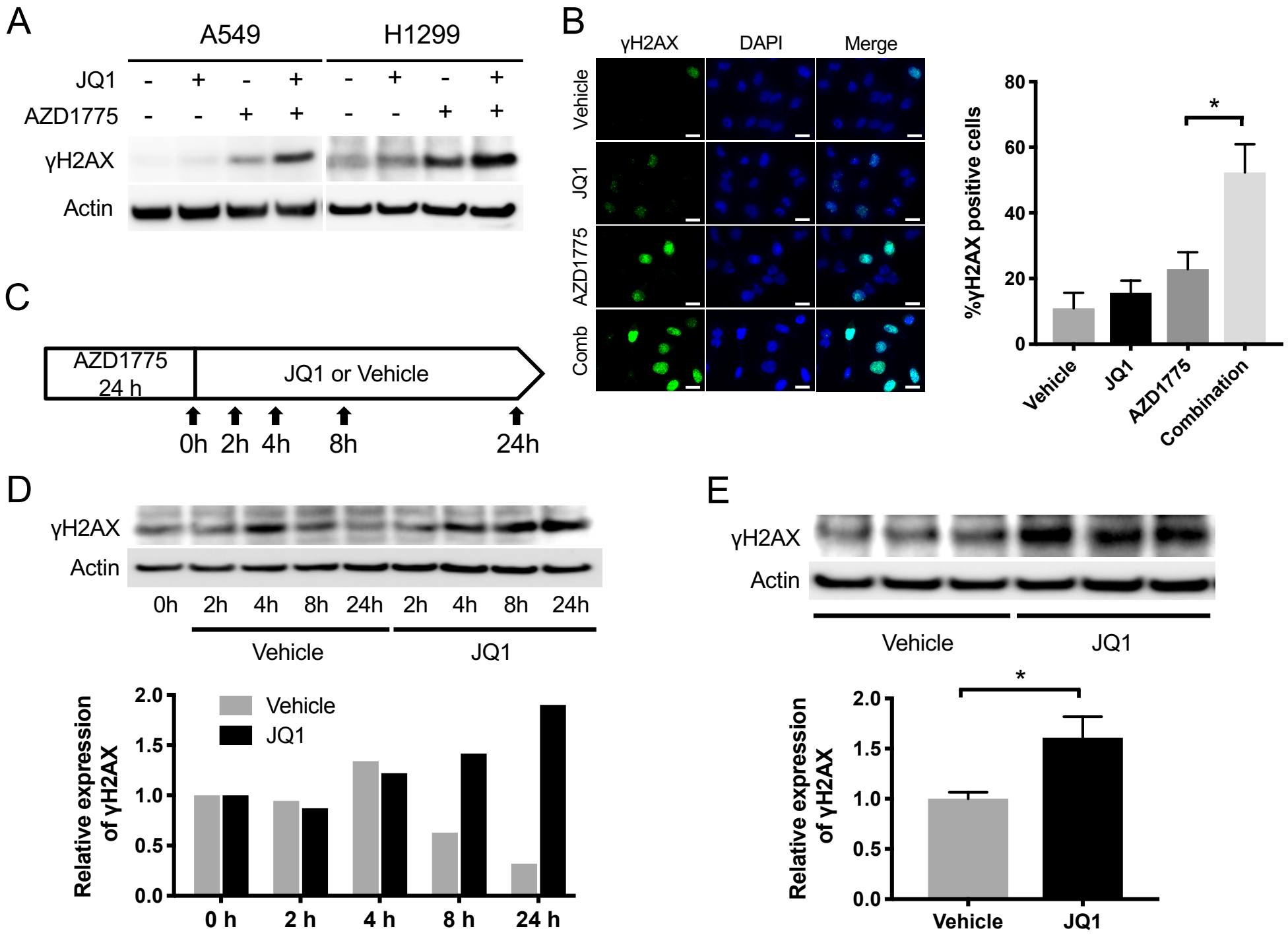
A
A549
H1299
JQ1
AZD1775
γH2AX
Actin
B
γH2AX
DAPI
Merge
Vehicle
JQ1
AZD1775
Comb
%γH2AX positive cells
Vehicle
JQ1
AZD1775
Combination
C
AZD1775
24 h
JQ1 or Vehicle
0h 2h 4h 8h 24h
D
γH2AX
Actin
0h 2h 4h 8h 24h 2h 4h 8h 24h
Vehicle
JQ1
Relative expression of γH2AX
Vehicle
JQ1
0 h 2 h 4 h 8 h 24 h
E
γH2AX
Actin
Vehicle
JQ1
Relative expression of γH2AX
Vehicle
JQ1

Figure 3.

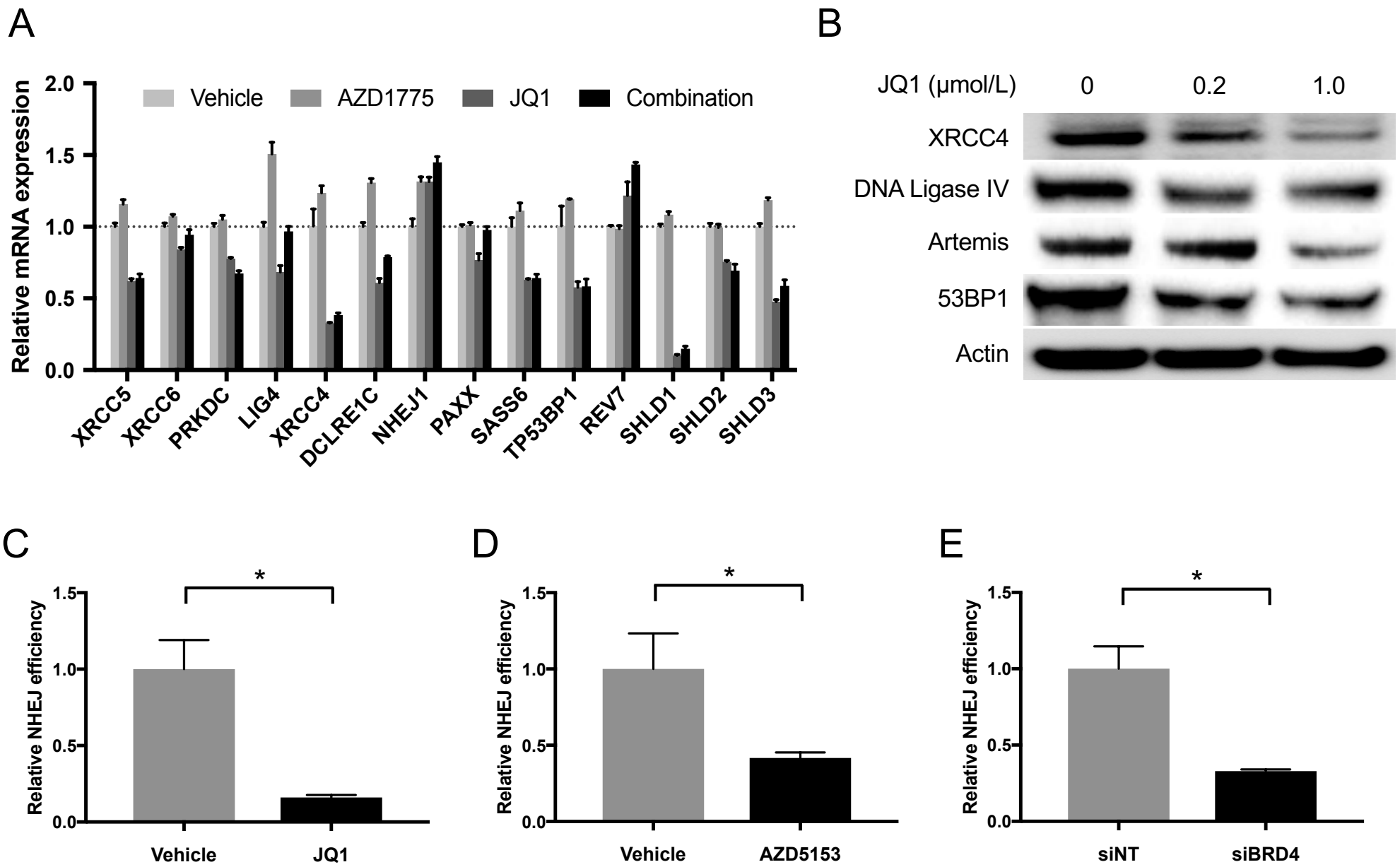
A
Vehicle
AZD1775
JQ1
Combination
Relative mRNA expression
2.0
1.5
1.0
0.5
0.0
XRCC5
XRCC6
PRKDC
LIG4
XRCC4
DCLRE1C
NHEJ1
PAXX
SASS6
TP53BP1
REV7
SHLD1
SHLD2
SHLD3
B
JQ1 (μmol/L)
0
0.2
1.0
XRCC4
DNA Ligase IV
Artemis
53BP1
Actin
C
Relative NHEJ efficiency
1.5
1.0
0.5
0.0
*
Vehicle
JQ1
D
Relative NHEJ efficiency
1.5
1.0
0.5
0.0
*
Vehicle
AZD5153
E
Relative NHEJ efficiency
1.5
1.0
0.5
0.0
*
siNT
siBRD4

Figure 4.

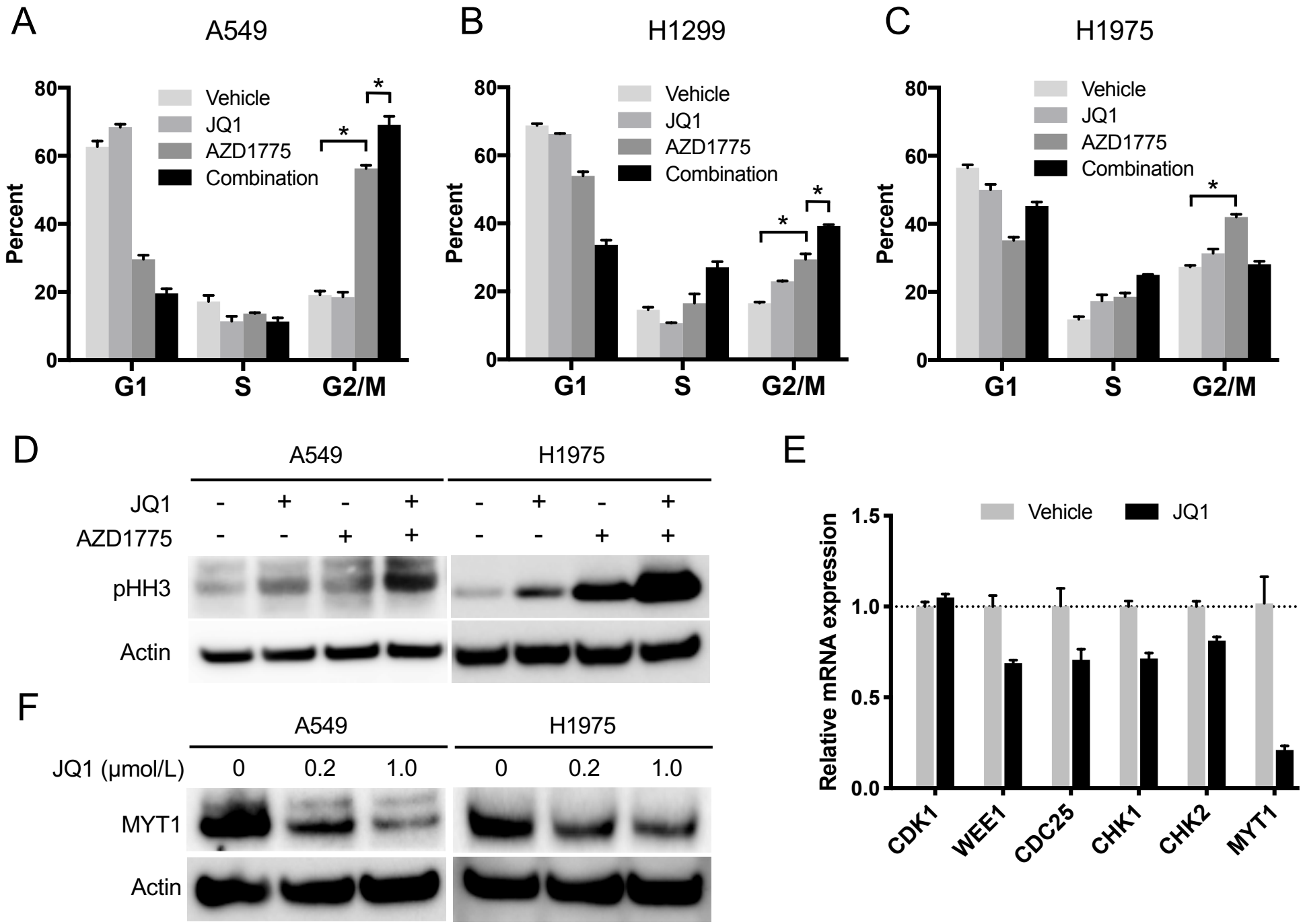
A
A549
B
H1299
C
H1975
Vehicle
JQ1
AZD1775
Combination
Percent
80
60
40
20
0
G1
S
G2/M
*
D
A549
H1975
JQ1
AZD1775
pHH3
Actin
E
Relative mRNA expression
1.5
1.0
0.5
0.0
CDK1
WEE1
CDC25
CHK1
CHK2
MYT1
F
JQ1 (μmol/L)
0
0.2
1.0
MYT1
Actin

Figure 5.

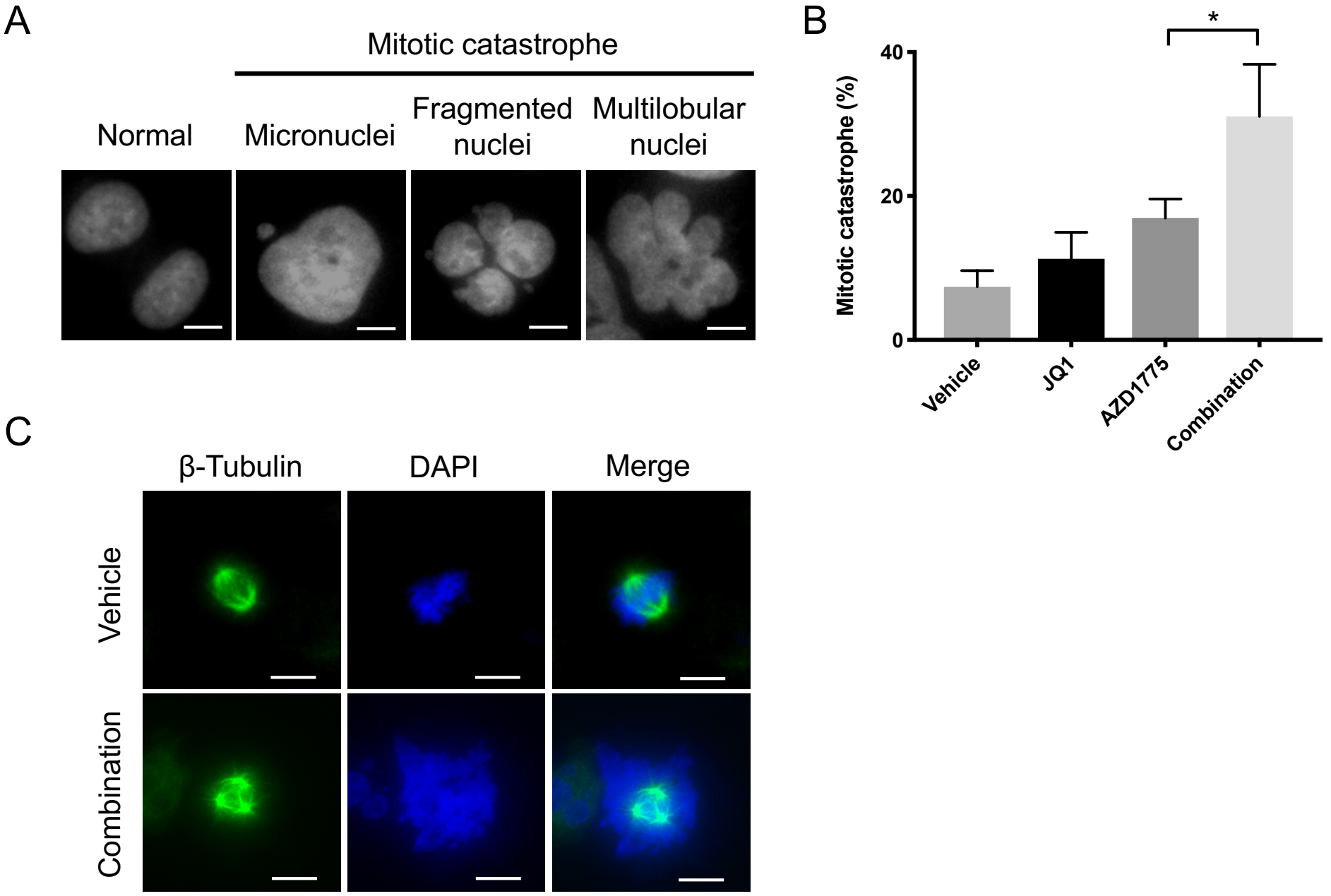
A
Mitotic catastrophe
Normal
Micronuclei
Fragmented nuclei
Multilobular nuclei
B
Mitotic catastrophe (%)
40
20
0
*
Vehicle
JQ1
AZD1775
Combination
C
β-Tubulin
DAPI
Merge
Vehicle
Combination

Figure 6.

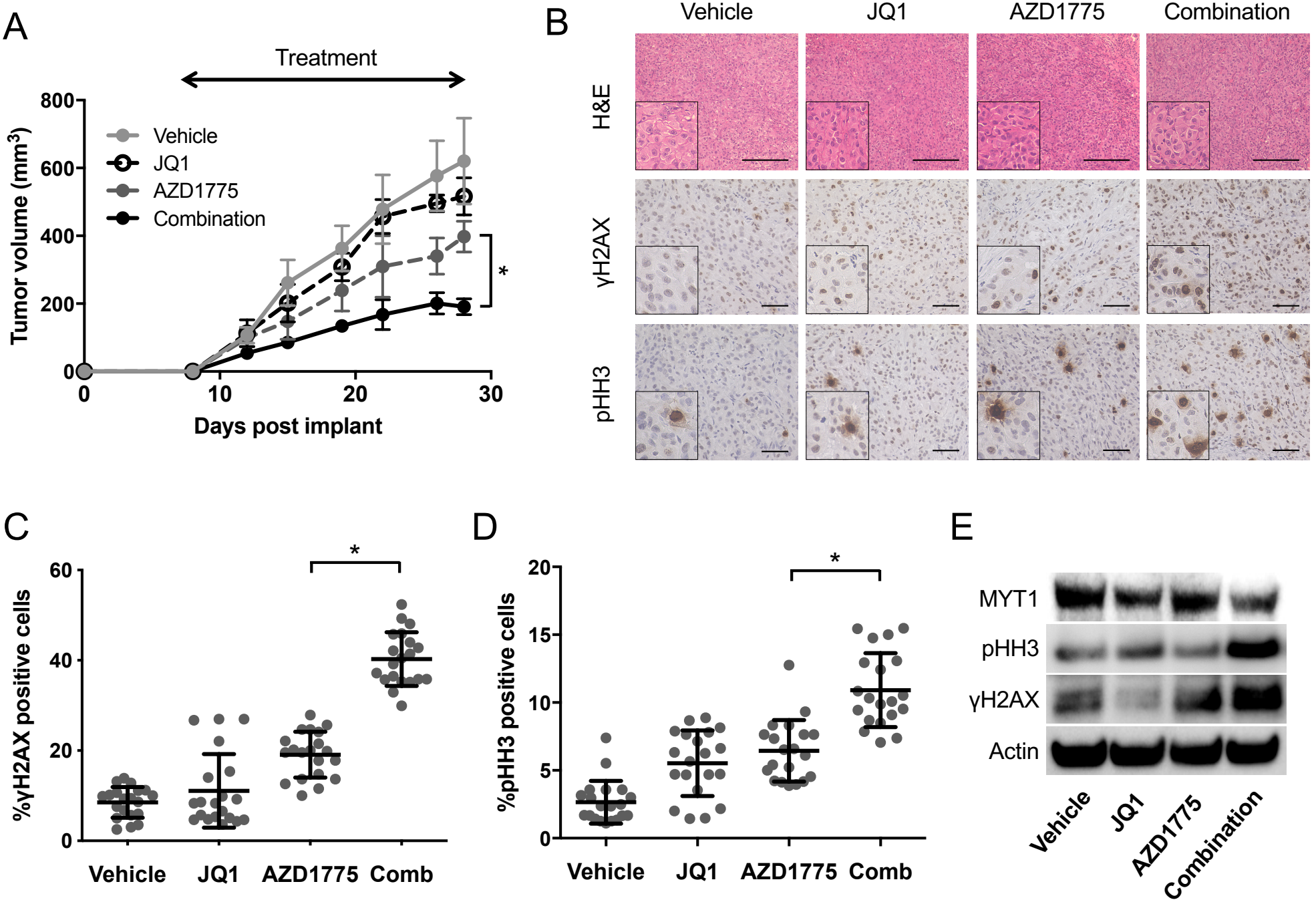
A
Treatment
Tumor volume (mm³)
800
600
400
200
0
Vehicle
JQ1
AZD1775
Combination
*
0
10
20
30
Days post implant
B
Vehicle
JQ1
AZD1775
Combination
H&E
γH2AX
pHH3
C
%γH2AX positive cells
60
40
20
0
*
Vehicle
JQ1
AZD1775
Comb
D
%pHH3 positive cells
20
15
10
5
0
*
Vehicle
JQ1
AZD1775
Comb
E
MYT1
pHH3
γH2AX
Actin
Vehicle
JQ1
AZD1775
Combination